Formation of hyperdeformed states by neutron emission from a dinuclear system

A. S. Zubov,[1] V. V. Sargsyan,[1,2] G. G. Adamian,[1,3] N. V. Antonenko,[1] and W. Scheid[4]
[1]*Joint Institute for Nuclear Research, RU-141980 Dubna, Russia*
[2]*Yerevan State University, 0025 Yerevan, Armenia*
[3]*Institute of Nuclear Physics, Tashkent 702132, Uzbekistan*
[4]*Institut für Theoretische Physik der Justus-Liebig-Universität, D-35392 Giessen, Germany*
(Received 5 November 2009; published 17 February 2010)

The hyperdeformed nuclei treated as dinuclear or quasimolecular configurations are suggested to be directly produced in heavy-ion reactions at bombarding energies near the Coulomb barrier. The excited dinuclear system formed in the entrance channel of the heavy-ion collision can be cooled down by neutron emission to be transformed into the hyperdeformed nuclear system. This transition from the excited dinuclear system to a hyperdeformed configuration is described within the statistical approach. The reactions ^{48}Ca + ^{124,128,130,132,134}Sn, ^{48}Ca + ^{136,138}Xe, ^{48}Ca + ^{137,138,140}Ba, ^{40}Ca + ^{83,84}Kr, ^{48}Ca + ^{83,84,86}Kr, ^{40,48}Ca + ^{40,48}Ca, ^{58,60}Ni + ^{58,60}Ni, and ^{40}Ca + ^{58}Ni are suggested for the population of hyperdeformed states. The production cross sections, quadrupole moments, and moments of inertia of hyperdeformed states formed in these reactions are calculated, and the optimal conditions for the experimental identification of such states are proposed.

DOI: 10.1103/PhysRevC.81.024607 PACS number(s): 25.70.Jj, 24.10.−i, 24.60.−k

I. INTRODUCTION

The evidence of low-spin hyperdeformed (HD) states in actinides has been experimentally established in induced fission reactions (n,f), (t,pf), and (d,pf) [1–3]. These shape isomer states are caused by a third minimum in the potential energy surfaces (PESs), which appears at very large quadrupole deformation parameters $\beta_2 \gtrsim 0.9$. Using the shell-model calculations, it was shown that the third minimum in the PESs of actinide nuclei belongs to rather a quasimolecular configuration of two touching nuclei (clusters) [4]. The validity of the cluster interpretation of the HD isomers was investigated in Refs. [5–8]. Based on the results of Refs. [7,8], one can be convinced that certain quasimolecular configurations with the dumb-bell shapes have the same quadrupole moments and moments of inertia as those measured for superdeformed (SD) and HD isomer states.

Up to now there has been little experimental information on the high-spin HD states of heavy nuclei. Evidence for HD bands in ^{152,153}Dy and ^{147}Gd was earlier reported in Ref. [9] with the reactions ^{120}Sn(^{37}Cl,$p\ xn$)^{152,153}Dy and ^{100}Mo(^{51}V, $p\ 3n$)^{147}Gd. The ridge structure, which consists of stretched $E2$ transitions found in a proton-selected γ-γ matrix in these reactions, suggested the existence of a HD prolate shape with a quadrupole deformation of $\beta_2 \geqslant 0.9$. But it was later shown in Ref. [10] that the candidates for HD states in ^{147}Gd and ^{152,153}Dy have no properties consistent with band structure. Thus, there is no experimental evidence that proton emission plays an important role in the population of HD states. Within semiphenomenological cranked Woods-Saxon and Nilsson approaches [11,12], the HD structures were predicted to become yrast states in ^{147}Gd and ^{152}Dy at spins $L = 80$ and 90, respectively.

In light α-particle nuclei, the similarity between HD and cluster-type states, i.e., quasimolecular states, was mentioned in Refs. [13–15]. In a fragment-fragment-γ (the γ rays are emitted from the fragments) triple coincidence experiment [16], the possibility of a preferential population of highly deformed bands in ^{56}Ni was investigated in the ^{28}Si + ^{28}Si reaction at an energy of a conjectured quasimolecular resonance with a spin $L = 38$. The possible occurrence of HD configurations was investigated in the ^{40}Ca and ^{56}Ni dinuclear systems formed in the ^{28}Si + ^{12}C and ^{28}Si + ^{28}Si reactions, respectively, by using the spectral properties of emitted light charged particles (p,d,t,α) [15]. In this experiment, two heavy fragments were detected in coincidence with a light charged particle associated with them. In Refs. [17–20], the extremely elongated nuclear shapes of light nuclei, for example, ^{24}Mg, ^{36}Ar, ^{56}Ni, and ^{60}Zn, have been treated as cluster states.

Investigations of the high-spin SD and HD rotational bands in different mass regions were performed with the cranked-shell and mean-field approaches using a few deformation parameters, and with cluster models in which the cluster degrees of freedom, taken properly, allow us to simplify the treatment of a nuclear system in the space of collective coordinates [22]. There have been many recent developments in the field of nuclear clusters including the ability to perform *ab initio* calculations of the light nuclei, such as Green's function Monte Carlo methods [23] and antisymmetrized molecular dynamics [22,24]. As known from the study of light nuclei ^{8}Be and ^{32}S, the highly deformed shape can be considered as a symmetric dimolecular shape rather than an ellipsoid. The semimicroscopic symmetry-adopted cluster approaches have been applied to predict the SD and HD states in light nuclei [20,21]. The calculations for heavy nuclei with the cluster models [8,25–28] have shown that the configurations with large quadrupole and octupole deformation parameters and the low-lying collective negative-parity states are strongly related to dinuclear clustering. With the cluster approach [8,27,28], the main properties of SD states in several isotopes of Pb and Hg have been described. In the cluster models [25,26], the charge (mass) asymmetry coordinate is fixed, and the main collective coordinate is the relative distance between the centers of

 ©2010 The American Physical Society

the clusters. Because of this, the clusters penetrate each other.

The indications of population of high-spin HD states in fusion-evaporation reactions with heavy ions have been discussed in Ref. [29]. In Refs. [8,12], it has been suggested to directly populate these states in heavy-ion collisions without going via the stage of compound-nucleus formation that is in accordance with the dinuclear interpretation of strongly deformed nuclear states. In this model, two clusters are in touching configuration. The relative distance between the centers of the clusters corresponds to the minimum of the nucleus-nucleus interaction potential and is larger than the sum of cluster radii. The overlapping of nuclei is hindered by a repulsive nucleus-nucleus interaction potential at smaller relative distances. The minimum of nucleus-nucleus potential energy contains the quasibound states with the energies below the potential barrier and with large half-lives. These states should be directly populated by tunneling through the entrance barrier including the centrifugal potential. In this case, the cold dinuclear system (DNS) is formed in the entrance channel of reaction. This DNS, if it lives quite a long time, can be treated as the HD state. The quadrupole moments of such a DNS with mass asymmetry $|\eta| = |A_1 - A_2|/(A_1 + A_2) \lesssim 0.6$ (A_1 and A_2 are the mass numbers of the DNS nuclei) are equal to or larger than the quadrupole moment of an ellipsoid with $\beta_2 = 0.9$ [7]. Asymmetric DNSs have relatively large octupole deformation. The experimental identification of the HD state can be obtained by measuring the consecutive collective rotational $E2$ transitions in the HD band in coincidence with the decay fragments of the DNS trapped in the HD minimum [8].

In the present paper, we use the dinuclear interpretation of the HD nuclear states and study a new possibility to populate the HD states directly in the entrance channel of heavy-ion reactions after the neutron emission. The bombarding energy is slightly larger than the Coulomb barrier. Taking neutron-rich isotopes as projectiles, one can lower the neutron binding energy and increase the probability of neutron emission from the DNS and, thus, produce the HD states with larger cross sections. Considering the wide isotopic composition of the colliding nuclei, the influence of the entrance channel on the dynamics of the formation of the cold DNS and on the possibility of emission of γ cascades which get trapped in the HD minimum will be analyzed. Optimal conditions for such experiments will be proposed.

II. FORMATION OF HYPERDEFORMED STATES IN HEAVY-ION COLLISIONS

A. Model

Our treatment is based on the cluster or molecular interpretation of strongly deformed nuclear states. This interpretation assumes that the DNS is formed after the colliding nuclei pass over the Coulomb barrier and come to the touching configuration. The DNS can evolve by diffusion in the relative distance R between the centers of nuclei and in the charge $\eta_Z = (Z_1 - Z_2)/(Z_1 + Z_2)$ and mass η asymmetry coordinates (Z_1 and Z_2 are the charge numbers of the DNS nuclei) [30–32]. The initial DNS with an excitation energy higher than the depth of the third potential minimum can be deexcited by the emission of a neutron, which competes with the diffusion in η_Z to more symmetric or asymmetric configurations and the diffusion to larger R (DNS decay or quasifission). The residue daughter DNS configuration can be cold enough and can live a long enough time to be interpreted as a HD state. Such a system has also the possibility of the emission of γ quanta between collective rotational states.

So, our model treats the formation and decay of the HD state as a three-step process. First, the excited initial DNS is formed in the entrance channel. Second, the cold DNS corresponding to HD state is produced by the emission of a neutron. Third, this rotating DNS emits γ quanta and/or reseparates into two fragments.

B. HD-state formation cross section

The cross section $\sigma_{\rm HD}(E_{\rm c.m.})$ for the formation of the HD state depends on the capture cross section or the capture probability $P_{\rm cap}$, which is related to the formation of excited initial DNS and the probability $P_{\rm HD}$ of transformation of this DNS into HD state (cold DNS):

$$\begin{aligned}\sigma_{\rm HD}(E_{\rm c.m.}) &= \sum_{L=L_{\rm min}}^{L_{\rm max}} \sigma_{\rm HD}(E_{\rm c.m.}, L) \\ &= \sum_{L=L_{\rm min}}^{L_{\rm max}} \frac{\pi\hbar^2}{2\mu E_{\rm c.m.}}(2L+1) \\ &\quad \times P_{\rm cap}(E_{\rm c.m.}, L) P_{\rm HD}(E_{\rm c.m.}, L). \end{aligned} \tag{1}$$

Here, $\sigma_{\rm HD}(E_{\rm c.m.}, L)$ is the partial cross section and $E_{\rm c.m.}$ is the bombarding energy in the center-of-mass system. As shown below, for each reaction there is a certain interval of angular momentum L from $L_{\rm min}$ to $L_{\rm max}$, where the value $\sigma_{\rm HD}$ is maximal, and there is a chance to observe the γ transitions between rotational states of the formed HD band. Out of this interval, the identification of HD states seems to be difficult.

C. DNS potential energy and nucleus-nucleus interaction potential

Under the assumption of a small overlap of the nuclei in the DNS, the potential energy of DNS is calculated as follows [30]:

$$U(R, \eta, \eta_Z, \beta_1, \beta_2, L) = B_1 + B_2 + V(R, \eta, \eta_Z, \beta_1, \beta_2, L), \tag{2}$$

where B_1 and B_2 are the mass excesses of the fragments at their ground states, and β_1 and β_2 are their quadrupole deformation parameters. The experimental values of B_1 and B_2 are used, if available, from Ref. [33]. Otherwise, we use the values from Ref. [34]. The quadrupole deformation parameters are taken from Refs. [34,35]. The nucleus-nucleus potential

$$\begin{aligned} &V(R, \eta, \eta_Z, \beta_1, \beta_2, L) \\ &= V_C(R, \eta_Z, \beta_1, \beta_2) + V_N(R, \eta, \beta_1, \beta_2) + V_{\rm rot}(\eta, \beta_1, \beta_2, L) \end{aligned} \tag{3}$$

in Eq. (2) is the sum of the Coulomb potential V_C, the nuclear potential V_N, and the centrifugal potential $V_{\rm rot} = \hbar^2 L(L+1)/(2\Im)$, where $\Im$ is the moment of inertia of the DNS formed (see Sec. III). In the entrance channel (the capture stage), $\Im = \mu R^2$, where μ is the reduced mass of relative motion. For the nuclear part, we use the double-folding formalism with the Skyrme-type effective density-dependent nucleon-nucleon interaction [6,30,31]. The densities of the nuclei are taken in the Woods-Saxon form with the nuclear radius parameter $r_0 = 1.15$ fm and the diffuseness parameter $a = 0.55$ fm [6]. Due to the sum of the repulsive Coulomb and centrifugal summands with the attractive nuclear one in Eq. (3), the nucleus-nucleus potential has a pocket with a minimum situated for pole-pole orientation at the distance $R = R_m \approx R_1(1 + \sqrt{5/(4\pi)}\beta_1) + R_2(1 + \sqrt{5/(4\pi)}\beta_2) + 0.5$ fm ($R_i = r_0 A_i^{1/3}$ fm). The position of the Coulomb barrier corresponds to $R = R_b \approx R_m + 1$ fm in the DNS considered. Then the depth of the potential pocket is $B_R^{\rm qf} = V(R_b, \eta, \eta_Z, \beta_1, \beta_2, L) - V(R_m, \eta, \eta_Z, \beta_1, \beta_2, L)$. The barrier $B_R^{\rm qf}$, called the quasifission barrier, prevents the DNS decay in the R coordinate. The DNS being cold can be trapped in the potential minimum during a time sufficient to emit the γ quanta between collective rotational states.

The nucleus-nucleus potential V as a function of R and the potential energy U at $R = R_m(\eta)$ as a function of Z_1 at different angular momenta L are presented in Fig. 1. For each η_Z, we minimized $U(R_m, \eta, \eta_Z, \beta_1, \beta_2, L)$ with respect to η. The values of barriers $B_R^{\rm qf}$ and B_{η_Z} are also shown. The evolution of the excited DNS is the DNS transition over the barrier $B_R^{\rm qf}$ in R (DNS decay) or over the barriers $B_{\eta_Z}^{\rm sym}$ and $B_{\eta_Z}^{\rm asym}$ in η_Z, in the direction to more symmetric and more asymmetric configurations, respectively. For reactions with $\eta_{Z_0} = 0$, like ^{40}Ca + ^{48}Ca, there is no barrier $B_{\eta_Z}^{\rm sym}$ but there are two equal barriers $B_{\eta_Z} = B_{\eta_Z}^{\rm asym}$, which prevent the diffusion of the DNS to positive and negative values of η_Z. The DNS should not spread in η_Z in order to have a larger cross section of the formation of certain HD state. While the depth $B_R^{\rm qf}$ of the potential pocket decreases with angular momentum L due to the growth of the repulsive centrifugal part of the nucleus-nucleus potential [Eq. (3)] and vanishes for $L > 90$ in the case of the considered DNS, the value of B_{η_Z} only slightly increases with L. At high angular momenta $L > 60$, in the case of ^{40}Ca + ^{48}Ca and of some other reactions, the potential energy of the DNS, normalized to the energy of the compound nucleus, is negative. This indicates that the complete fusion becomes energetically denied.

D. Capture probability

To calculate the value $P_{\rm cap}$, we use the formalism of the reduced density matrix [36] taking into account the influence of dissipation and fluctuations in the relative distance coordinate R. At bombarding energies near the Coulomb barrier, one can visualize a capture as a process in which a part of the initial Gaussian wave packet populates the nucleus-nucleus potential pocket behind the Coulomb barrier. By solving the quantum master equation for the R degree of freedom, we find the diagonal elements $\rho(t, R)$ of the reduced density matrix in the coordinate representation [36]. The capture probability is defined with the ratio

$$P_{\rm cap}(E_{\rm c.m.}, L) = \frac{\int_{-\infty}^{R_b} \rho(\tau, R) dR}{\int_{R_b}^{\infty} \rho(t = 0, R) dR}, \qquad (4)$$

where R_b defines the position of the Coulomb barrier, and the projectile is assumed to approach the target from the right side. The value of τ determines the time of capture. For the trajectory (the mean value of relative distance R) above the Coulomb barrier, the larger part of the Gaussian wave packet is trapped in the potential pocket or in a quasibound state. Then, there is a decay in R from this state. The value of τ is thus defined as the time within which the quasistationary flux from the potential pocket sets in. When the trajectory does not cross the top of the barrier, the value of τ is defined as the time of returning back to the starting point taken at $R = R_b + 1$ fm. The details of calculation of $P_{\rm cap}$ are presented in Ref. [36].

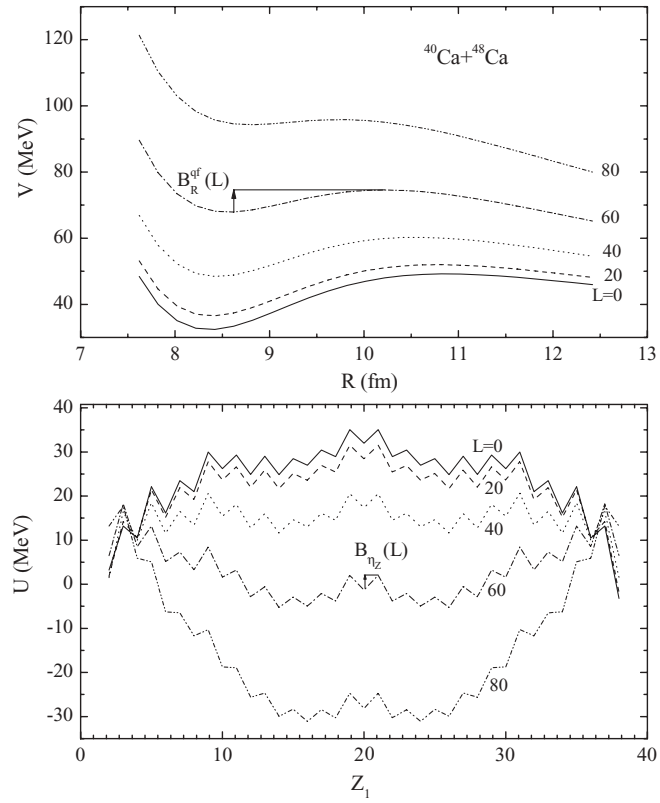

FIG. 1. Dependencies of the nucleus-nucleus potential V on R (upper part) and of the potential energies U of the DNS at $R = R_m(\eta)$ on charge number Z_1 of one DNS nucleus (lower part) for the reaction ^{40}Ca + ^{48}Ca. The calculated results are presented for $L = 0$, 20, 40, 60, 80 as labeled on the curves. The value of U is normalized to the energy of the rotating compound nucleus.

E. DNS excitation energy

The excitation energy of the initial DNS, formed in the entrance channel of the reaction at $R = R_m$, $\eta_Z = \eta_{Z_0}$ and $\eta = \eta_{\rm in}$, is $E_{\rm in}^* = E_{\rm c.m.} - V(R_m, \eta_{\rm in}, \eta_{Z_0}, \beta_1, \beta_2, L)$. After the N/Z equilibrium at given η_{Z_0} is reached, which seems to be a fast process, the value of η is changed from $\eta_{\rm in}$ to η_0.

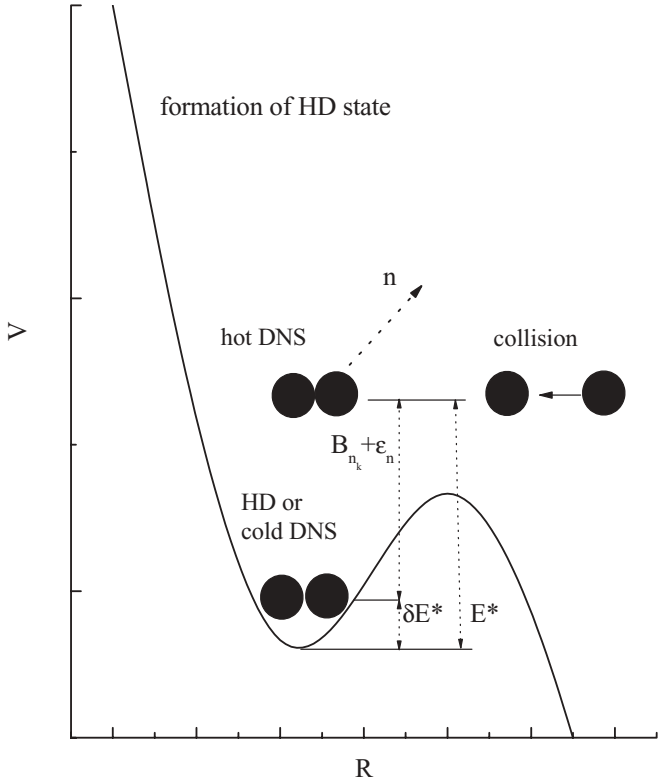

FIG. 2. Scheme of formation of the HD state in the entrance channel of nuclear reaction.

The excitation energy of the DNS increases by the value of $\Delta U_{\rm in} = U(R_m, \eta_{Z_0}, \eta_{\rm in}) - U(R_m, \eta_{Z_0}, \eta_0)$. Because in the reactions considered the distribution of the DNS in η at given η_{Z_0} is strongly peaked at η_0, we disregard the distribution of the DNS in η in the vicinity of η_0 [32], where the DNS potential energy is minimal.

F. Neutron emission and transformation of DNS into HD state

The proposed mechanism of the population of HD states is schematically presented in Fig. 2. To form the quasibound cold state of DNS, which is treated here as the HD state, the excitation energy $E^* = E^*_{\rm in} + \Delta U_{\rm in}$ of the DNS should be reduced to the value $E^*_{\rm HD} < \delta E^*$, where $\delta E^* = 0.2$ MeV is assumed in our calculation. This decrease of the DNS excitation energy can be provided by the emission of a neutron which carries away the energy $B_{n_k} + \epsilon_n$, where ϵ_n is the kinetic energy of the neutron and B_{n_k} the neutron separation energy, $E^*_{\rm HD} = E^* - B_{n_k} - \epsilon_n$. The index $k = 1$ or 2 corresponds to the DNS nucleus. Here, we take into consideration that the neutron can be evaporated from each nucleus of the DNS. As shown in Ref. [37], in the case of emission of one neutron, which we consider here, the neutron spectrum is close to the Maxwellian distribution. Using the Maxwellian form of neutron spectrum, the probability w_{n_k} to emit the neutron with kinetic energies in the interval from $E^* - B_{n_k} - \delta E^*$ to $E^* - B_{n_k}$ and to cool the excited DNS to $E^*_{\rm HD} < \delta E^*$ is estimated as

$$w_{n_k}(E^*, B_{n_k}, \delta E^*) = \frac{\int_{E^*-B_{n_k}-\delta E^*}^{E^*-B_{n_k}} \epsilon_n \exp[-\epsilon_n/T_{n_k}(E^*)]/[T_{n_k}(E^*)]^2 d\epsilon_n}{\int_0^{E^*-B_{n_k}} \epsilon_n \exp[-\epsilon_n/T_{n_k}(E^*)]/[T_{n_k}(E^*)]^2 d\epsilon_n}, \quad (5)$$

where $T_{n_k}(E^*) = \sqrt{E^* \frac{A_k}{A_1+A_2}/a(A_k)}$ and $a(A_k)$ are the temperature and the level density parameter of the kth nucleus of the DNS, respectively.

In the statistical approach, the evolution of the excited DNS is prescribed by the competition between the neutron emission from the system and the DNS transition over the quasifission barrier $B^{\rm qf}_R$ in R or over the barriers $B^{\rm sym}_{\eta_Z}$ and $B^{\rm asym}_{\eta_Z}$ in η_Z, in the direction to more symmetric and more asymmetric configurations, respectively. The transition over the barrier $B^{\rm asym}_{\eta_Z}$ opens the way to fusion [30–32], because the DNS approaches the compound nucleus with increasing η_Z. Taking into account the competition of different deexcitation channels [the factor $P_{n_k}(E^*, B_{n_k}, L)$], the probability $P_{\rm HD}(E_{\rm c.m.}, L)$ of formation of the HD state by neutron emission from the excited initial DNS is defined as

$$P_{\rm HD} = \sum_{k=1}^{2} P_{n_k}(E^*, B_{n_k}, L) w_{n_k}(E^*, B_{n_k}, \delta E^*), \quad (6)$$

$$P_{n_k} = \frac{\Gamma_{n_k}(E^*, \eta_{Z_0}, L)}{\Gamma_n(E^*, \eta_{Z_0}, L) + \Gamma^{\rm qf}_R(E^*, \eta_{Z_0}, L) + \Gamma^{\rm sym}_{\eta_Z}(E^*, \eta_{Z_0}, L) + \Gamma^{\rm asym}_{\eta_Z}(E^*, \eta_{Z_0}, L)},$$

where Γ_{n_k} is the width of neutron emission from the kth nucleus of the DNS, $\Gamma_n = \Gamma_{n_1} + \Gamma_{n_2}$, and $\Gamma^{\rm qf}_R$, $\Gamma^{\rm sym}_{\eta_Z}$, and $\Gamma^{\rm asym}_{\eta_Z}$ are the widths of transitions over the barriers $B^{\rm qf}_R$, $B^{\rm sym}_{\eta_Z}$, and $B^{\rm asym}_{\eta_Z}$, respectively. The heights and curvatures $\hbar\omega^{\rm qf}_R$, $\hbar\omega^{\rm sym}_{\eta_Z}$, and $\hbar\omega^{\rm asym}_{\eta_Z}$ of these barriers are defined using the DNS potential energy, defined by Eq. (2). In the considered reactions, the typical values of $\hbar\omega^{\rm qf}_R$ and $\hbar\omega^{\rm sym,asym}_{\eta_Z}$ are about 2.5 and 1 MeV, respectively. The widths of each channel (neutron emission or transitions over the barriers) strongly depend on the intrinsic level density of the DNS in the corresponding states; see the Appendix, Eqs. (A4) and (A5).

III. NUCLEAR PROPERTIES OF HD STATES

A. Moment of inertia, electric quadrupole moment, $E2$-transition time

Since the experimental identification of HD states is going to be based on the registration of collective rotational $E2$

transitions, it is necessary to define the nuclear properties of the HD states as moments of inertia and quadrupole moments. We calculate these values using the cluster approach proposed in Ref. [7], where the HD states are treated as the cold DNS configurations. Since the overlap of nuclei in the DNS is quite small, the DNS moment of inertia $\Im$ is calculated in the sticking limit as

$$\Im = k_0(\Im_1 + \Im_2 + \mu R^2). \tag{7}$$

For large angular momenta L, the moments of inertia $\Im_i$ $(i = 1, 2)$ of the DNS nuclei are obtained in the rigid body approximation:

$$\begin{aligned} \Im_i &= \frac{1}{5} m_0 A_i \left(a_i^2 + b_i^2\right), \\ a_i &= R_{0i}\left(1 - \frac{\beta_i^2}{4\pi}\right)\left(1 + \sqrt{\frac{5}{4\pi}}\beta_i\right), \\ b_i &= R_{0i}\left(1 - \frac{\beta_i^2}{4\pi}\right)\left(1 - \sqrt{\frac{5}{16\pi}}\beta_i\right). \end{aligned} \tag{8}$$

As known from the experimental study, the moments of inertia of strongly deformed nuclear states are very close to 85% of those in the rigid body limit [12]. We also set $k_0 = 0.85$ in our calculations.

The charge multipole moments of the DNS are calculated as ($\lambda \leqslant 2$)

$$Q_{\lambda\mu}^{(c)} = \sqrt{\frac{16\pi}{2\lambda + 1}} \int \rho^{(c)}(\mathbf{r}) r^{\lambda} Y_{\lambda\mu}(\Omega) d\mathbf{r}, \tag{9}$$

where the charge density $\rho^{(c)}(\mathbf{r})$ is written as the sum of densities of each nucleus: $\rho^{(c)}(\mathbf{r}) = \rho_1^{(c)}(\mathbf{r}) + \rho_2^{(c)}(\mathbf{r})$. Assuming axially symmetric nuclear shapes, one can obtain the following expression for the multipole moments of the DNS in the c.m. system:

$$\begin{aligned} Q_{\lambda 0}^{(c)} = Q_{\lambda}^{(c)} = &\sum_{\substack{\lambda_1 = 0 \\ \lambda_1 + \lambda_2 = \lambda}}^{\lambda} (-1)^{\lambda} \frac{\lambda!}{\lambda_1! \lambda_2!} \\ &\times \left[(-1)^{\lambda_1} A_2^{\lambda_1} Q_{\lambda_2}^{(c)}(1) + A_1^{\lambda_1} Q_{\lambda_2}^{(c)}(2)\right] \frac{R^{\lambda_1}}{A^{\lambda_1}}, \end{aligned} \tag{10}$$

where the multipole moments $Q_{\lambda_2}^{(c)}(i)$ $(i = 1, 2)$ of the DNS nuclei are calculated in their centers of mass. Then the electric quadrupole moment of the DNS is

$$Q_2^{(c)} = 2e \frac{A_2^2 Z_1 + A_1^2 Z_2}{A^2} R^2 + Q_2^{(c)}(1) + Q_2^{(c)}(2). \tag{11}$$

Using the values of $\Im$ and $Q_2^{(c)}$, we obtain the energy $E_\gamma(L \to L - 2)$ and the time $T_\gamma(L)$ of the collective $E2$ transition between the rotational states with angular momenta L and $L - 2$ as [35]

$$\begin{aligned} E_\gamma(L \to L - 2) &= L(L + 1)/(2\Im) - (L - 2)(L - 1)/(2\Im), \\ T_\gamma(L) &= \frac{408.1}{5/(16\pi)\left(Q_2^{(c)}\right)^2 [E_\gamma(L \to L - 2)]^5}, \end{aligned} \tag{12}$$

where E_γ is in units of keV, $Q_2^{(c)}$ in $10^2(e\ \mathrm{fm}^2)$, and T_γ in s.

B. Method of identification of HD band

One can propose the experimental method of identification of the HD states by measuring rotational γ quanta in the HD band in coincidence with the decay into fragments constituting the HD states formed in the entrance channel with fixed η_{Z_0}. This means that the properties of the formed cold system must fulfill the following conditions:

$$T_\gamma \lesssim T_R \lesssim T_{\eta_Z}, \tag{13}$$

where T_R and T_{η_Z} are the tunneling times through the barrier in the R and η_Z coordinate, respectively, which can be estimated using the parabolic approximation for the PES as ($i = R, \eta_Z$, $j =$ qf, asym)

$$T_i = \frac{2\pi}{\Omega_i^j}\left(1 + \exp\frac{2\pi B_i^j}{\hbar\omega_i^j}\right), \tag{14}$$

where Ω_i^j and ω_i^j are the corresponding frequencies in the minimum of the potential energy and on the barrier, respectively, and B_i^j are the heights of barriers for the daughter DNS after the neutron emission. $B_{\eta_Z}^j$ is the minimal value of the barrier which prevents the evolution of DNS in η_Z to the direction of more symmetric or more asymmetric configurations. For the asymmetric reactions considered, $B_{\eta_Z}^{\mathrm{asym}} < B_{\eta_Z}^{\mathrm{sym}}$, and the tunneling through the barrier $B_{\eta_Z}^{\mathrm{sym}}$ can be neglected. In the case of symmetric reactions, there are two equal barriers $B_{\eta_Z} = B_{\eta_Z}^{\mathrm{asym}}$ to the direction of asymmetric configurations, and the number of barrier assaults per time is twice larger than for the asymmetric configuration, and this should be taken into consideration in formula (14). In the considered reactions, the typical values of $\hbar\omega_R^{\mathrm{qf}}$ and $\hbar\omega_{\eta_Z}^{\mathrm{asym}}$ are about 2.5–2.7 and 1 MeV, respectively.

Using the rates $\Lambda_{\gamma,R,\eta_Z} = \hbar/T_{\gamma,R,\eta_Z}$ of different competing processes (collective γ transition in the HD band and tunneling in R and η_Z) from the HD minimum in the PES and $\Lambda_{\mathrm{tot}} = \Lambda_\gamma + \Lambda_R + \Lambda_{\eta_Z}$, one can estimate the probability of the emission of x γ quanta from the HD state just before its decay in R as

$$P_{x\gamma R} = \frac{\Lambda_R(L - 2x)}{\Lambda_{\mathrm{tot}}(L - 2x)} \prod_{k=0}^{x-1} \frac{\Lambda_\gamma(L - 2k)}{\Lambda_{\mathrm{tot}}(L - 2k)}. \tag{15}$$

Then the cross section of emission of at least x γ quanta(um) from the HD state before its decay in R can be calculated as

$$\sigma_{x\gamma R} = \sum_{L=L_{\min}}^{L_{\max}} \sigma_{\mathrm{HD}}(E_{\mathrm{c.m.}}, L) \sum_{x'=x}^{[L/2]} P_{x'\gamma R}, \tag{16}$$

where $[L_{\min}/2] \geqslant x$. Since the internal angular momentum of the even-odd daughter DNS is small in comparison to L, it was not taken into consideration. Since the detection of γ quanta in coincidence with the decay products of the HD state provides the identification of the HD state, the cross section $\sigma_{x\gamma R}$ is called the identification cross section. Measuring the consecutive $E2$ γ transitions, one can determine the moments of inertia and electric quadrupole moments of the analyzed HD states.

The cross section of the HD-state decay in R without γ emission ($x = 0$) is

$$\sigma_{0\gamma R} = \sum_{L=L_{\min}}^{L_{\max}} \sigma_{\rm HD}(E_{\rm c.m.}, L)\frac{\Lambda_R(L)}{\Lambda_{\rm tot}(L)}. \quad (17)$$

IV. RESULTS OF CALCULATIONS

A. HD-state formation cross section

The isotopic dependence of the cross sections for the formation of the HD state in the reaction ^{48}Ca + ^{A_2}Sn at $L = 40$–50 is presented in Fig. 3. While the barriers $B_R^{\rm qf}$ and $B_{\eta_Z}^{\rm sym}$ increase with A_2, the value of $B_{\eta_Z}^{\rm asym}$ decreases. The influence of this decrease on the probability of neutron emission is not compensated by the decrease of neutron binding energy until $A_2 = 132$, at which the minimization over N/Z leads to the DNS ^{50}Ca + ^{130}Sn. Since the difference of neutron binding energies of Ca isotopes is more than 2 MeV [$B_n(^{48}\text{Ca}) = 8.8$ MeV and $B_n(^{50}\text{Ca}) = 6.42$ MeV], there are the increases of P_n and $\sigma_{\rm HD}$ at $A_2 = 132$. At $A_2 = 134$, the configuration with the minimal potential energy is ^{50}Ca + ^{132}Sn. Because of the influence of the closed neutron shell $N = 82$ in the tin isotope, the neutron emission becomes more suppressed in this case and $\sigma_{\rm HD}$ becomes smaller than $\sigma_{\rm HD}$ at $A_2 = 132$.

B. HD-state identification cross section

The condition (13) sufficiently restricts the interval of angular momenta at which it is possible to identify HD states, because the characteristic times of different processes depend on L. As seen from Eq. (12), the value of T_γ mainly depends on L through E_γ. The angular-momentum dependence of T_{R,η_Z} are defined by the angular-momentum dependence of the corresponding barriers. While the barrier in η_Z is weakly affected by the change of L ($B_{\eta_Z}^{\rm sym}$ slowly increases and $B_{\eta_Z}^{\rm asym}$ slowly decreases with increasing L), the value of quasifission barrier $B_R^{\rm qf}$ decreases much greater with increasing contribution of the repulsive centrifugal part of the nucleus-nucleus potential (3) (see also Fig. 1). For example, the values T_γ, T_R, and T_{η_Z} as the functions of L are presented in Fig. 4 for the HD states formed in the entrance channel of reactions ^{48}Ca + ^{142}Ce, ^{60}Ni + ^{60}Ni, and ^{48}Ca + ^{140}Ba. The condition $T_\gamma \lesssim T_R$ is satisfied only in some interval of L. At very small angular momentum, the time of the $E2$ transition becomes enormous due to the small values of $E_\gamma(L \to L-2)$; and at very large L, the value of T_R becomes very small because the quasifission barrier vanishes. In addition, the values of $B_{\eta_Z}^{\rm sym,asym}$ in this interval of L should be quite large to provide the condition $T_R \lesssim T_{\eta_Z}$. Thus, one can hope to identify the HD states by measuring the consecutive rotational $E2$ transitions in the HD band in coincidence with the decay fragments at $20 < L < 60$ and $40 < L < 70$ in the

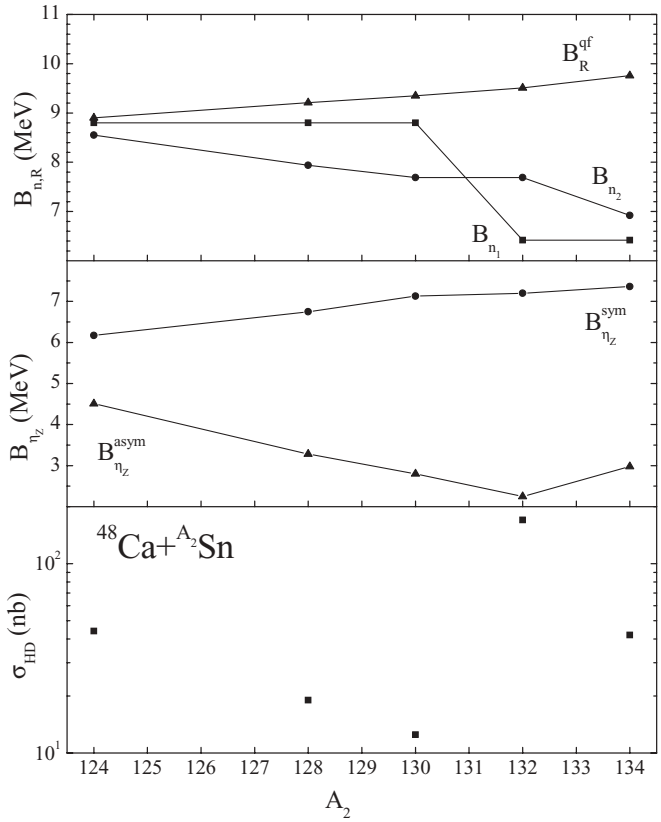

FIG. 3. Isotopic dependence of neutron binding energies and quasifission barriers $B_R^{\rm qf}$ (upper part), barriers $B_{\eta_Z}^{\rm sym}$ and $B_{\eta_Z}^{\rm asym}$ (middle), and cross sections for the formation of the HD state (lower) in the reactions ^{48}Ca + ^{A_2}Sn at $L = 40$–50.

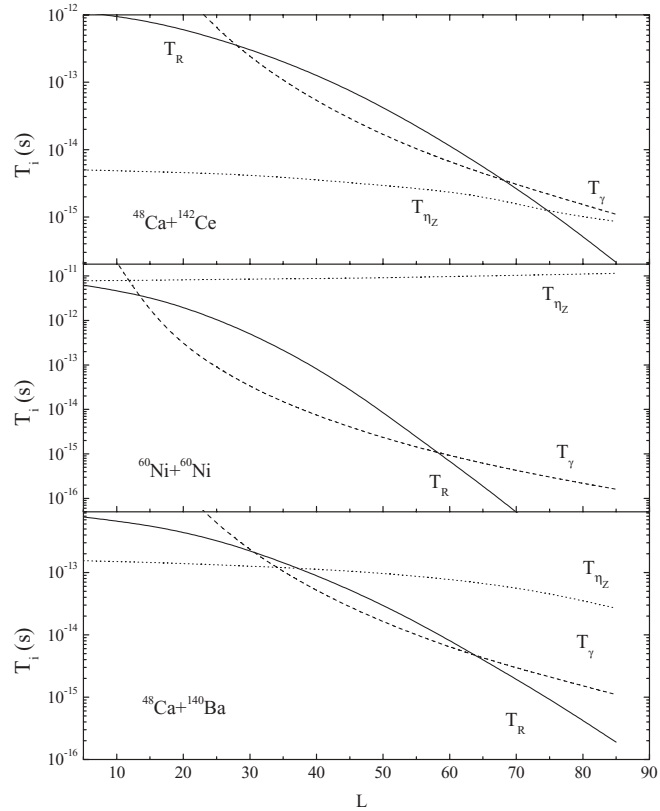

FIG. 4. Time of collective $E2$-transition and tunneling times through the barriers in R and η_Z for the HD states formed in the entrance channel of the indicated reactions as the functions of angular momentum L.

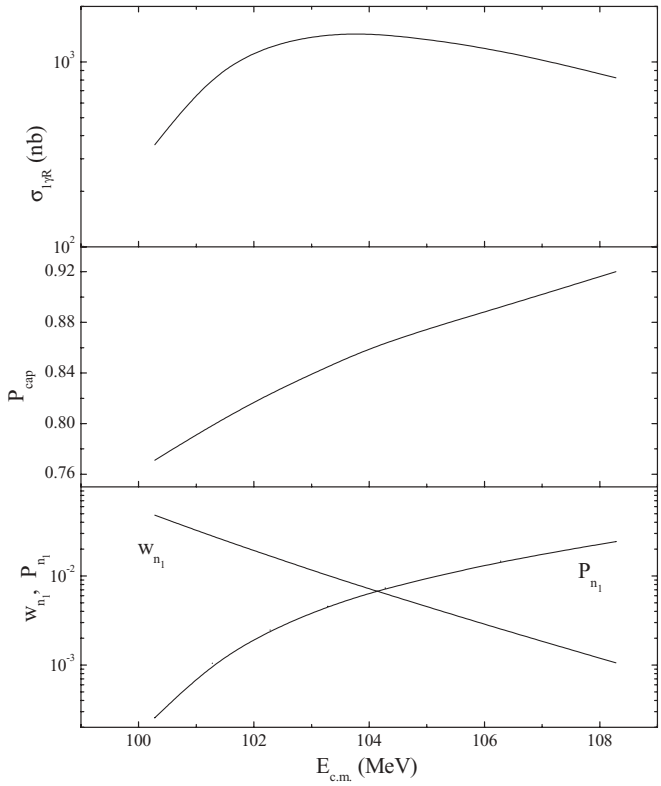

FIG. 5. Probabilities P_{n_1} and w_{n_1} (lower part), probability of capture $P_{\rm cap}$ (middle), and identification cross section $\sigma_{1\gamma R}$ of the HD state formed in the ^{60}Ni + ^{60}Ni reaction at $L = 30$–40 (upper) as functions of the bombarding energy $E_{\rm c.m.}$.

reactions ^{60}Ni + ^{60}Ni and ^{48}Ca + ^{140}Ba, respectively; but it will be difficult to identify the HD states at any angular momenta in the ^{48}Ca + ^{142}Ce reaction (Fig. 4).

Examples of the dependencies of $\sigma_{1\gamma R}$ and the factors $P_{\rm cap}$, P_{n_1}, and w_{n_1} on the bombarding energy $E_{\rm c.m.}$ are shown in Fig. 5. The capture probability slowly increases with $E_{\rm c.m.}$ and does not affect much the location of the maximum of the function $\sigma_{1\gamma R}(E_{\rm c.m.})$. This location is mainly determined by P_{n_1} and w_{n_1}. While P_{n_1} increases, w_{n_1} decreases with increasing $E_{\rm c.m.}$. The final curve representing the function $\sigma_{1\gamma R}(E_{\rm c.m.})$ has a maximum, which is usually about 8–10 MeV higher than the value of the entrance Coulomb barrier $V(R_b, \eta, \eta_Z, \beta_1, \beta_2, L)$. The location of this maximum gives us the optimal bombarding energy for each considered reaction. With increasing angular momentum, the value of $\sigma_{\rm HD}$ decreases because of the decrease of $B_R^{\rm qf}$ with increasing L, but this dependence is also strongly shadowed by the conditions in Eq. (13). This leads to a very individual picture of the dependence $\sigma_{x\gamma R}$ on L for each reaction.

C. Optimal reactions for the formation and identification of HD state

We calculate the moments of inertia, electric quadrupole moments, optimal bombarding energy, range of angular momenta, and cross sections of formation $\sigma_{\rm HD}$ and identification $\sigma_{x\gamma R}$ for the HD states formed in the entrance channel of the reactions given in Tables I–IV. The choice of the reactions is based on the following criteria: (1) In the entrance channel of the reaction, the DNS should have a local potential minimum which is populated; and after neutron emission, a cold quasibound state, treated here as hyperdeformed, is formed. (2) There should exist the range of angular momenta satisfying the conditions of Eq. (13). (3) Neutron-rich projectiles and targets are preferable in order to increase the probability of neutron emission from the initial DNS. However, only those nuclei are considered that can be experimentally accelerated with quite a large intensity. (4) The estimated identification cross section of the HD state should be suitable for the present experimental setups.

As one can see from Tables I–IV, the combination of all these conditions leads to a complicated isotopic dependence of the value of $\sigma_{x\gamma R}$. Symmetric reactions lead to larger $\sigma_{x\gamma R}$ if more neutron-rich nuclei are used. One can compare, for example, the reactions ^{40}Ca + ^{40}Ca and ^{48}Ca + ^{48}Ca. For the treated asymmetric reactions with ^{48}Ca, there are no such marked trends.

TABLE I. Moments of inertia, electric quadrupole moments, range of angular momenta, optimal bombarding energies, and cross sections $\sigma_{\rm HD}$ and $\sigma_{x\gamma R}$ ($x = 0, 1, 2, 3$) calculated for the HD states formed in the entrance channel of the reactions ^{40}Ca + ^{83,84}Kr and ^{48}Ca + ^{83,84,86}Kr.

Reactions	$\Im$ ($\hbar^2$/MeV)	$Q_2^{(c)}$ $10^2(e\ {\rm fm}^2)$	$L_{\rm min} < L < L_{\rm max}$	$E_{\rm c.m.}$ (MeV)	$\sigma_{\rm HD}$ (nb)	$\sigma_{0\gamma R}$ (nb)	$\sigma_{1\gamma R}$ (nb)	$\sigma_{2\gamma R}$ (nb)	$\sigma_{3\gamma R}$ (nb)
^{48}Ca + ^{83}Kr	90.6	28.4	$60 < L < 70$	106.5	78	1.1	1.1	0.5	0.2
			$70 < L < 80$	113.3	32	2.7	2.4	1.3	0.73
^{48}Ca + ^{84}Kr	88.7	27.4	$60 < L < 70$	112.3	192	1.7	1.3	0.53	0.21
			$70 < L < 80$	119.1	109	18	10	3.6	1.3
^{48}Ca + ^{86}Kr	91	27.6	$50 < L < 60$	104.8	620	0.97	1.7	1.1	0.76
			$60 < L < 70$	110.6	430	5.6	10	6.6	4.1
			$70 < L < 80$	117.2	240	17	34	23	16
^{40}Ca + ^{83}Kr	86.9	30.3	$60 < L < 70$	114.7	24	6.1	6.4	3.5	2.1
			$70 < L < 80$	121.6	18	1.1	2	1.3	0.83
^{40}Ca + ^{84}Kr	86.2	29.6	$60 < L < 70$	114.6	50	2.7	2.4	1.1	0.5
			$70 < L < 80$	121.6	19	6.8	4.6	2	0.88

TABLE II. Same as Table I, but for the reactions ^{40,48}Ca + ^{40,48}Ca, ^{58,60}Ni + ^{58,60}Ni, and ^{40}Ca + ^{58}Ni.

Reactions	$\Im$ ($\hbar^2$/MeV)	$Q_2^{(c)}$ $10^2(e\ \mathrm{fm}^2)$	$L_{\min} < L < L_{\max}$	$E_{\mathrm{c.m.}}$ (MeV)	σ_{HD} (nb)	$\sigma_{0\gamma R}$ (nb)	$\sigma_{1\gamma R}$ (nb)	$\sigma_{2\gamma R}$ (nb)	$\sigma_{3\gamma R}$ (nb)
^{40}Ca + ^{40}Ca	38.1	13.9	$20 < L < 30$	69.7	1×10^4	1.7	123	122	120
			$30 < L < 40$	76.7	7.3×10^3	16	110	100	96
			$40 < L < 50$	86	2.8×10^3	290	250	130	75
^{40}Ca + ^{48}Ca	44.6	14.8	$50 < L < 60$	84.6	3.4×10^3	360	200	72	26
			$60 < L < 70$	96	1.5×10^3	1.4×10^3	40	24	6.1
^{48}Ca + ^{48}Ca	51.5	15.6	$40 < L < 50$	66.5	5.9×10^4	94	23	4.6	1.1
			$50 < L < 60$	75.1	3.2×10^4	3.8×10^3	2.4×10^3	970	390
			$60 < L < 70$	85.2	1.1×10^4	9.7×10^4	1.3×10^3	270	83
^{58}Ni + ^{58}Ni	83.0	31.3	$20 < L < 30$	104.4	2.2×10^3	570	1.7×10^3	1.2×10^3	760
			$30 < L < 40$	107.6	1.1×10^3	142	450	350	270
			$40 < L < 50$	111.8	600	260	340	210	140
			$50 < L < 60$	116.9	250	190	59	17	6.2
^{58}Ni + ^{60}Ni	86.2	32.1	$20 < L < 30$	103.1	710	110	420	320	230
			$30 < L < 40$	106.4	540	73	380	320	270
			$40 < L < 50$	110.2	330	87	220	170	130
			$50 < L < 60$	115.2	160	100	61	28	14
^{60}Ni + ^{60}Ni	89.3	32.9	$20 < L < 30$	99.9	2.2×10^3	200	1.4×10^3	1.2×10^3	980
			$30 < L < 40$	103.3	2×10^3	160	1.4×10^3	1.4×10^3	1.2×10^3
			$40 < L < 50$	106.7	1×10^3	160	770	650	570
			$50 < L < 60$	111.5	510	220	280	180	120
^{40}Ca + ^{58}Ni	56.9	21	$10 < L < 20$	81.5	580	0.98	61	59	54
			$20 < L < 30$	85.6	420	0.33	46	46	45
			$30 < L < 40$	89.2	170	0.36	20	19	19
			$40 < L < 50$	95.4	49	0.95	6.8	6.2	5.8
			$50 < L < 60$	103	9.5	2.6	3	1.8	1.2

Comparing the calculated values of $\sigma_{1\gamma R}$, $\sigma_{2\gamma R}$, and $\sigma_{3\gamma R}$, one can see that for some reactions these cross sections decrease rather slowly with the number of emitted γ quanta, which means that an articulate rotational band of the formed HD state can be experimentally observed. For example, in the reaction ^{60}Ni + ^{60}Ni at an initial value of $L = 40$–50, the calculated value of $\sigma_{10\gamma R}$ is 260 nb.

TABLE III. Same as Table I, but for the reactions ^{48}Ca + ^{124,128,130,132,134}Sn.

Reactions	$\Im$ ($\hbar^2$/MeV)	$Q_2^{(c)}$ $10^2(e\ \mathrm{fm}^2)$	$L_{\min} < L < L_{\max}$	$E_{\mathrm{c.m.}}$ (MeV)	σ_{HD} (nb)	$\sigma_{0\gamma R}$ (nb)	$\sigma_{1\gamma R}$ (nb)	$\sigma_{2\gamma R}$ (nb)	$\sigma_{3\gamma R}$ (nb)
^{48}Ca + ^{124}Sn	122.9	34.1	$20 < L < 30$	119.7	150	34	120	86	55
			$30 < L < 40$	122.3	100	12	92	80	69
			$40 < L < 50$	124.2	54	5.8	48	42	38
			$50 < L < 60$	127.8	25	4.3	21	18	15
^{48}Ca + ^{128}Sn	125.7	34.9	$20 < L < 30$	118.4	110	15	51	36	22
			$30 < L < 40$	120.5	52	3.7	31	27	23
			$40 < L < 50$	123.3	19	0.48	10	10	9.5
			$50 < L < 60$	126.8	6	0.61	4.3	3.8	3.4
^{48}Ca + ^{130}Sn	128.6	34.5	$40 < L < 50$	127	13	0.57	4.6	4.3	3
			$50 < L < 60$	130.4	5.8	0.41	2.6	2.2	1.9
			$60 < L < 70$	134.5	2.4	0.34	1.4	1.1	0.9
^{48}Ca + ^{132}Sn	129.9	34.5	$60 < L < 70$	133	23	3.8	6.4	4	2.5
			$70 < L < 80$	136.6	19	7.2	8.5	4.8	2.8
			$80 < L < 90$	141.8	8.3	5.6	2.5	0.89	0.36
^{48}Ca + ^{134}Sn	129.8	33.8	$50 < L < 60$	122.7	13	0.5	4.9	4.4	3.8
			$60 < L < 70$	126.7	5.6	0.47	2.7	2.3	2.1
			$70 < L < 80$	131.3	2.1	0.43	1.3	0.97	0.77

TABLE IV. Same as Table I, but for the reactions ^{48}Ca + ^{136,138}Xe and ^{48}Ca + ^{137,138,140}Ba.

Reactions	$\Im$ ($\hbar^2$/MeV)	$Q_2^{(c)}$ $10^2(e\ \mathrm{fm}^2)$	$L_{\min} < L < L_{\max}$	$E_{\mathrm{c.m.}}$ (MeV)	σ_{HD} (nb)	$\sigma_{0\gamma R}$ (nb)	$\sigma_{1\gamma R}$ (nb)	$\sigma_{2\gamma R}$ (nb)	$\sigma_{3\gamma R}$ (nb)
^{48}Ca + ^{136}Xe	135.1	36.9	$20 < L < 30$	126.3	110	33	73	45	21
			$30 < L < 40$	128.3	48	7.4	40	33	27
			$40 < L < 50$	130.7	17	2.4	15	13	11
			$50 < L < 60$	134.1	8.5	1.5	7	5.8	4.9
^{48}Ca + ^{138}Xe	138.2	37.3	$20 < L < 30$	119.7	640	150	380	250	130
			$30 < L < 40$	121.6	280	32	220	190	150
			$40 < L < 50$	126.2	130	15	110	94	83
			$50 < L < 60$	129.3	66	8.4	55	48	42
			$60 < L < 70$	133	27	5.7	21	17	14
^{48}Ca + ^{137}Ba	136.4	37.6	$20 < L < 30$	131.7	75	52	19	4	0.65
			$30 < L < 40$	133.6	41	21	19	8.5	3.4
			$40 < L < 50$	136.2	29	2.3	26	22	18
			$50 < L < 60$	139.4	15	7.1	7.2	4.5	3.3
^{48}Ca + ^{138}Ba	136.2	37.2	$20 < L < 30$	131	93	64	27	6.2	1.1
			$30 < L < 40$	133.9	53	26	26	12	5.4
			$40 < L < 50$	135.4	24	1.7	22	19	15
			$50 < L < 60$	138.5	9.4	4.4	4.9	3.2	2.4
^{48}Ca + ^{140}Ba	138	36.8	$40 < L < 50$	134	84	25	35	19	10
			$50 < L < 60$	137.1	69	21	37	23	14
			$60 < L < 70$	140.8	23	12	11	5.3	2.9

V. SUMMARY

Using the cluster approach, we proposed a model of the HD-state formation in the entrance channel of a heavy-ion reaction at bombarding energies near the Coulomb barrier. The initial DNS, formed at an excitation energy of about 18–20 MeV, then can be deexcited by the emission of a neutron to the cold quasibound state which is identical to the HD state. The neutron emission from the DNS, which competes with the quasifission and diffusion of the initial DNS to more symmetric or asymmetric configurations, is described by using a statistical approach. One can identify the HD state by measuring the consecutive collective rotational $E2$ transitions in coincidence with the decay fragments of the DNS constituting the HD configuration. Such requirements to the experiment restrict the set of possible reactions and the optimal range of angular momenta.

We propose to consider the reactions ^{48}Ca + ^{124,128,130,132,134}Sn, ^{48}Ca + ^{136,138}Xe, ^{48}Ca + ^{137,138,140}Ba, ^{40}Ca + ^{83,84}Kr, ^{48}Ca + ^{83,84,86}Kr, ^{40,48}Ca + ^{40,48}Ca, ^{58,60}Ni + ^{58,60}Ni, and ^{40}Ca + ^{58}Ni as good candidates for the production and experimental identification of the HD states. The estimated identification cross sections $\sigma_{x\gamma R}$ for the HD states formed in these reactions are of the order of 1 nb to 2.5 μb for optimal bombarding energies and range of angular momenta.

ACKNOWLEDGMENTS

This work was supported by DFG and RFBR. The MTA-JINR, Polish-JINR, and IN2P3-JINR Cooperation programs are gratefully acknowledged.

APPENDIX

The intrinsic level density of the DNS with the excitation energy E^* is defined in Ref. [38] with the folding procedure

$$\begin{aligned}\rho_{\mathrm{DNS}}(E^*, A_1, A_2, J_1, J_2) &= \int_0^{E^*}\int_0^{E^*} \rho_1(E_1, A_1, J_1)\rho_2(E_2, A_2, J_2) \\ &\quad \times \delta(E_1 + E_2 - E^*)dE_1dE_2 \\ &= \int_0^{E^*} \rho_1(E_1, A_1, J_1)\rho_2(E^* - E_1, A_2, J_2)dE_1, \quad \text{(A1)}\end{aligned}$$

where $J_{1,2} = L\Im_{1,2}/\Im$ are the spins of the DNS nuclei. The intrinsic level densities ρ_1 and ρ_2 of the DNS nuclei are calculated using the Fermi-gas model [39]

$$\rho_i(E_i^*, A_i, J_i) = \frac{2J_i + 1}{24\sqrt{2}\sigma_i^3 a_i^{1/4}(E_i^* - \delta_i - E_{\mathrm{rot}})^{5/4}} \times \exp\{2\sqrt{a_i(E_i^* - \delta_i - E_{\mathrm{rot}})}\}, \quad \text{(A2)}$$

where $\sigma_i^2 = 6\overline{m_i^2}\sqrt{a_i(E^* - \delta_i - E_{\mathrm{rot}})}/\pi^2$ and $E_{\mathrm{rot}} = J_i(J_i + 1)/(2a_i\sigma_i^2)$. The pairing correction δ_i is $24/\sqrt{A_i}$, $12/\sqrt{A_i}$, and 0 MeV for even-even, odd, and odd-odd nuclei, respectively. The average projection of angular momentum of the single-particle states is estimated as $\overline{m_i^2} \approx 0.24A_i^{2/3}$. In our calculations, we take the level density parameter $a_i = (0.114A_i + 0.098A_i^{2/3})[1 + \delta W_i(1 - \exp[-0.051(E_i^* - \delta_i)])/(E_i^* - \delta_i)]$ MeV^{-1} [40] for all DNS nuclei considered. Here, δW_i is the microscopical correction to the nuclear-mass

formula [34]. Since the damping of the microscopical effects is taken into account in the level density parameter, we disregard it in the potential energy [41]. One can see [32] that the definition (A1) corresponds to the thermal equilibrium in the DNS.

For a parabolic approximation of the barriers in R and η_Z, the probabilities of transitions through the corresponding barriers are ($i = R, \eta_Z$, $j =$ qf, sym, asym) [32]

$$R_i^j(E^*, \eta_{Z_0}, L) = \int_0^{E^*-B_i^j(L)} \frac{\rho_{\rm DNS}\left(E^* - B_i^j(L) - \epsilon, A_1, A_2, J_1, J_2\right)d\epsilon}{1 + \exp\frac{2\pi[\epsilon + B_i^j(L) - E^*]}{\hbar\omega_i^j(L)}}. \quad \text{(A3)}$$

The widths of decay in R and spreading in η_Z are defined through the probabilities R_i^j of these processes as

$$\Gamma_i^j(E^*, \eta_{Z_0}, L) = \frac{R_i^j(E^*, \eta_{Z_0}, L)}{2\pi\rho_{\rm DNS}(E^*, A_1, A_2, J_1, J_2)}. \quad \text{(A4)}$$

The probability of neutron emission is written as in Ref. [32]

$$R_{n_k}(E^*, \eta_{Z_0}, L) = \sum_{J_k^d} \int_0^{E^*-B_{n_k}} \rho_{\rm DNS}(E^* - B_{n_k} - \epsilon, A_k - 1, A_{k'}, J_k^d, J_{k'}) \times T_{J_k^d}(A_k - 1, \epsilon)d\epsilon,$$

$$T_{J_k^d} = \sum_{S=|J_k^d-1/2|}^{J_k^d+1/2} \sum_{l=|J_k-S|}^{J_k+S} T_l(A_k - 1, \epsilon), \quad \text{(A5)}$$

where $k \neq k'$ and J_k^d is the spin of kth nucleus of the DNS after emission of a neutron. The value of R_{n_k} can be calculated by using the neutron binding energy B_{n_k}, the level density $\rho_{\rm DNS}(E^* - B_{n_k} - \epsilon, A_k - 1, A_{k'}, J_k^d, J_{k'})$ of the daughter DNS. The transition coefficients $T_{J_k^d}(A_k - 1, \epsilon)$ are calculated as in Ref. [42]. The neutron binding energies are taken from Ref. [33], if available, or from the theoretical predictions [34]. The neutron emission width is given as

$$\Gamma_{n_k}(E^*, \eta_{Z_0}, L) = \frac{R_{n_k}(E^*, \eta_{Z_0}, L)}{2\pi\rho_{\rm DNS}(E^*, A_1, A_2, J_1, J_2)}. \quad \text{(A6)}$$

[1] B. B. Back, H. C. Britt, J. D. Garett, and O. Hansen, Phys. Rev. Lett. **28**, 1707 (1972).
[2] F. F. Baumann and K. Th. Brinkmann, Nucl. Phys. **A502**, 271 (1989).
[3] A. Krasznahorkay *et al.*, Phys. Lett. **B461**, 15 (1999); Phys. Rev. Lett. **80**, 2073 (1998).
[4] S. Cwiok, W. Nazarewicz, J. X. Saladin, W. Plociennik, and A. Johnson, Phys. Lett. **B322**, 304 (1994).
[5] G. G. Adamian, N. V. Antonenko, R. V. Jolos, S. P. Ivanova, and A. K. Nasirov, in *International Conference on Nuclear Structure and Nuclear Reactions at Low and Intermediate Energies*, E4-93-58, Dubna, 1993, p. 217.
[6] G. G. Adamian, N. V. Antonenko, R. V. Jolos, S. P. Ivanova, and O. I. Melnikova, Int. J. Mod. Phys. E **5**, 191 (1996).
[7] T. M. Shneidman, G. G. Adamian, N. V. Antonenko, S. P. Ivanova, and W. Scheid, Nucl. Phys. **A671**, 119 (2000).
[8] G. G. Adamian, N. V. Antonenko, N. Nenoff, and W. Scheid, Phys. Rev. C **64**, 014306 (2001); in *Proceedings of the Symposium on Cluster Aspects of Quantum Many-Body Systems*, edited by K. Kato *et al.* (World Scientific, Singapore, 2002), p. 215; G. G. Adamian, A. V. Andreev, N. V. Antonenko, N. Nenoff, W. Scheid, and T. M. Shneidman, Heavy Ion Phys. **19**, 87 (2003); Acta Phys. Pol. B **34**, 2147 (2003); G. G. Adamian, N. V. Antonenko, and W. Scheid, Fizika B **12**, 21 (2003); S. N. Kuklin, G. G. Adamian, N. V. Antonenko, and W. Scheid, Int. J. Mod. Phys. E **17**, 2020 (2008).
[9] A. Galindo Uribarri *et al.*, Phys. Rev. Lett. **71**, 231 (1993); G. Viesti *et al.*, Phys. Rev. C **51**, 2385 (1995); D. R. LaFosse *et al.*, Phys. Rev. Lett. **74**, 5186 (1995).
[10] D. R. LaFosse *et al.*, Phys. Rev. C **54**, 1585 (1996); M. Lunardon *et al.*, *ibid.* **56**, 257 (1997); M. Aïche *et al.*, Eur. Phys. J. A **6**, 121 (1999); V. Rizzi *et al.*, *ibid.* **7**, 299 (2000).
[11] J. Dudek, T. Werner, and L. L. Riedinger, Phys. Lett. **B211**, 252 (1988).
[12] S. Åberg and L.-O. Jönsonn, Annu. Rev. Nucl. Part. Sci. **40**, 439 (1990); S. Åberg, Nucl. Phys. **A557**, 17 (1993); Z. Phys. A **349**, 205 (1994).
[13] N. Cindro, J. Phys. G **4**, L23 (1978); N. Cindro and W. Greiner, *ibid.* **9**, L175 (1983).
[14] W. Greiner, J. Y. Park, and W. Scheid, *Nuclear Molecules* (World Scientific, Singapore, 1995).
[15] S. J. Sanders, A. Szanto de Toledo, and C. Beck, Phys. Rep. **311**, 487 (1999); C. Beck *et al.*, in *Proceedings of the International Conference on Nuclear Reactions*, Varenna, Italy, 2000 (Ricerca Scientifica ed Educazione Permanente, Milano, 2000), p. 407.
[16] R. Nouicer *et al.*, Phys. Rev. C **60**, 041303(R) (1999).
[17] A. Morsad, F. Haas, C. Beck, and R. M. Freemann, Z. Phys. A **338**, 61 (1991); C. Beck *et al.*, Phys. Rev. C **63**, 014607 (2000); M. Rousseau *et al.*, *ibid.* **66**, 034612 (2002); C. Beck *et al.*, Heavy Ion Phys. **18**, 297 (2005); F. Haas, *ibid.* **18**, 279 (2005).
[18] W. von Oertzen, V. Zherebchevsky, B. Gebauer, Ch. Schulz, S. Thummerer, D. Kamanin, G. Royer, and Th. Wilpert, Phys. Rev. C **78**, 044615 (2008); W. von Oertzen *et al.*, Eur. Phys. J. A **36**, 279 (2008).
[19] C. Beck *et al.*, Phys. Rev. C **80**, 034604 (2009).
[20] W. Sciani, Y. Otani, A. Lepine-Szily, E. A. Benjamim, L. C. Chamon, R. L. Filho, J. Darai, and J. Cseh, Phys. Rev. C **80**, 034319 (2009); J. Cseh, J. Darai, W. Sciani, Y. Otani, A. Lepine-Szily, E. A. Benjamim, L. C. Chamon, and R. L. Filho, *ibid.* **80**, 034320 (2009).
[21] J. Cseh, G. Levai, A. Ventura, and L. Zuffi, Phys. Rev. C **58**, 2144 (1998); J. Cseh, A. Algora, J. Darai, and P. O. Hess, *ibid.* **70**, 034311 (2004).
[22] M. Freer, Rep. Prog. Phys. **70**, 2149 (2007).
[23] R. B. Wiringa, S. C. Pieper, J. Carlson, and V. R. Pandharipande, Phys. Rev. C **62**, 014001 (2000).
[24] Y. Kanada En'yo and H. Horiuchi, Prog. Theor. Phys. **142**, 205 (2001).

[25] G. Royer and F. Haddad, J. Phys. G **21**, 339 (1995).
[26] B. Buck, A. C. Merchant, and S. M. Perez, Phys. Rev. C **61**, 014310 (1999).
[27] G. G. Adamian, N. V. Antonenko, R. V. Jolos, Yu. V. Palchikov, and W. Scheid, Phys. Rev. C **67**, 054303 (2003).
[28] G. G. Adamian, N. V. Antonenko, R. V. Jolos, Yu.V. Palchikov, W. Scheid, and T. M. Shneidman, Nucl. Phys. **A734**, 433 (2003); Phys. Rev. C **69**, 054310 (2004).
[29] B. Herskind *et al.*, Phys. Scr. **T125**, 108 (2006); Acta Phys. Pol. B **38**, 1421 (2007).
[30] G. G. Adamian, N. V. Antonenko, and W. Scheid, Nucl. Phys. **A678**, 24 (2000).
[31] G. G. Adamian, N. V. Antonenko, and W. Scheid, Phys. Rev. C **68**, 034601 (2003).
[32] A. S. Zubov, G. G. Adamian, N. V. Antonenko, S. P. Ivanova, and W. Scheid, Eur. Phys. J. A **33**, 223 (2007).
[33] G. Audi, A. M. Wapstra, and C. Thibault, Nucl. Phys. **A729**, 337 (2003).
[34] P. Möller *et al.*, At. Data Nucl. Data Tables **59**, 185 (1995).
[35] S. Raman, C. W. Nestor Jr., and P. Tikkanen, At. Data Nucl. Data Tables **78**, 1 (2001).
[36] V. V. Sargsyan, A. S. Zubov, Z. Kanokov, G. G. Adamian, and N. V. Antonenko, Phys. At. Nucl. **72**, 425 (2009); V. V. Sargsyan, Z. Kanokov, G. G. Adamian, N. V. Antonenko, and W. Scheid, Phys. Rev. C **80**, 034606 (2009).
[37] D. Hilscher *et al.*, Phys. Rev. C **20**, 576 (1979).
[38] A. J. Cole, *Statistical Modes for Nuclear Decay* (IOP Publishing, Bristol, UK, 2000).
[39] A. Ignatyuk, K. K. Istekov, and G. N. Smirenkin, Sov. J. Nucl. Phys. **29**, 875 (1975).
[40] A. S. Iljinov *et al.*, Nucl. Phys. **A543**, 517 (1992).
[41] A. S. Zubov, G. G. Adamian, N. V. Antonenko, S. P. Ivanova, and W. Scheid, Eur. Phys. J. A **23**, 249 (2005); Phys. Rev. C **65**, 024308 (2002).
[42] S. G. Mashnik, A. J. Sierk, and K. K. Gudima, arXiv:nucl-th/0208048 (2002).